# Privatization of biofilm matrix in structurally heterogeneous biofilms

Simon B. Otto[1,*], Marivic Martin[1,2,*], Daniel Schäfer[2], Raimo Hartmann[3], Knut Drescher[3,4], Susanne Brix[5], Anna Dragoš[1,#] & Ákos T. Kovács[1,#]

[1] Bacterial Interactions and Evolution Group, Department of Biotechnology and Biomedicine, Technical University of Denmark, 2800 Kongens Lyngby, Denmark

[2] Terrestrial Biofilms Group, Institute of Microbiology, Friedrich Schiller University Jena, 07743 Jena, Germany

[3] Max Planck Institute for Terrestrial Microbiology, 35043 Marburg, Germany

[4] Department of Physics, Philipps-Universität Marburg, 35037 Marburg, Germany

[5] Disease Systems Immunology Group, Department of Biotechnology and Biomedicine, Technical University of Denmark, 2800 Kongens Lyngby, Denmark

* Contributed equally

[#] Corresponding authors: Ákos T. Kovács and Anna Dragoš

Bacterial Interactions and Evolution Group, Technical University of Denmark, 2800 Kongens Lyngby, Denmark; atkovacs@dtu.dk (ÁTK) and adragos@dtu.dk (AD)

Keywords: *Bacillus subtilis*, biofilm, phenotypic heterogeneity, structural heterogeneity, exopolysaccharide

**ABSTRACT**

The self-produced biofilm provides beneficial protection for the encased cells, but the costly production of matrix components makes producer cells susceptible to cheating by non-producing individuals. Despite detrimental effects of non-producers, biofilms can be heterogeneous, with isogenic non-producers being a natural consequence of phenotypic differentiation processes. In *Bacillus subtilis*, the expression of the two major matrix components of the biofilm, the amyloid fiber protein TasA and exopolysaccharides (EPS), is heterogeneous with cells demonstrating different expressive inclinations. This raises questions regarding matrix gene expression dynamics during biofilm development and the impact of phenotypic non-producers on biofilm robustness. Here, we show that biofilms are structurally heterogeneous and can be separated into strongly and weakly associated clusters. We reveal that spatiotemporal changes in structural heterogeneity correlate with matrix gene expression, with TasA playing a key role in biofilm integrity and timing of development. We show that the matrix remains partially privatized by the producer subpopulation, where cells tightly stick together even when exposed to shear stress. Our results support previous findings on the existence of 'weak points' in seemingly robust biofilms as well as on the key role of linkage proteins in biofilm formation. Furthermore, we provide a starting point for investigating the privatization of common goods within isogenic populations.

**SIGNIFICANCE STATEMENT**

Biofilms are communities of bacteria protected by a self-produced extracellular matrix. The detrimental effects of non-producing individuals on biofilm development raise questions about the dynamics between community members, especially when isogenic non-producers exist within wild-type populations. We asked ourselves whether phenotypic non-producers impact biofilm robustness, and where and when this heterogeneity of matrix gene expression occurs.

Based on our results we propose that the matrix remains partly privatized by the producing subpopulation, since producing cells stick together when exposed to shear stress. The important role of linkage proteins in robustness and development of the structurally heterogeneous biofilm provides an entry into studying the privatization of common goods within isogenic populations.

## INTRODUCTION

Biofilms are communities of tightly associated microorganisms encased in a self-produced extracellular matrix (1). This matrix provides shielding against biotic factors, such as antibiotics, and abiotic factors, such as shear stress (2–4). As components of the biofilm matrix are costly to produce and they can be shared within the population, matrix producers are potentially susceptible to social cheating, where non-producing mutants benefit from productive community members (5–7). This 'tragedy of the commons' principle, in which non-participating users cannot be excluded from the use of common goods (6, 8, 9), has already been demonstrated for *Pseudomonas fluorescens*, for which exploitation by an evolved non-producer resulted in biofilm collapse (10). Alternatively, production of the matrix components may not be easily exploitable if there is limited sharing, low cost of production, or the spatial assortment of cells within the biofilm (11, 12). Finally, long-term cheating on matrix production may have evolutionary consequences for the producers, changing the phenotypic heterogeneity pattern of matrix expression within the population (13).

Although so-called ‘cheating’ is traditionally associated with loss-of-function mutation in matrix genes, phenotypic non-producers (cells in the so-called OFF state) can be an intrinsic part of clonal wild-type populations (14–16). For instance in *Bacillus subtilis,* a probiotic and plant growth-promoting rhizobacteria strain (17, 18), the aforementioned phenotypic heterogeneity is fundamental to biofilm development, with individual cells exhibiting different tendencies to differentiate or express motility determinants (19). Pellicle biofilm formation in *B. subtilis* includes aerotaxis-driven loss of motility and subsequent adherent extracellular matrix production (20, 21). This differentiation of motile cells, becoming matrix-producing cells and spores, is not terminal, with genetically identical cells being able to alter their gene expression (22). While exploitability of extracellular matrix by non-producing mutants has been extensively studied, social interactions between clonal matrix producers and non-producers in

biofilms have been explored less. According to Hamilton's rule, altruistic sharing of public goods can easily evolve within isogenic populations, by means of inclusive fitness benefits (5). In other words, as long as the recipient carries the cooperative gene, cooperation should be evolutionary stable in the absence of additional stabilizing mechanisms (23–26).

Still, it is not clear to what extent the matrix is shared between phenotypically heterogeneous producers and non-producers, whether the presence of a non-producing subpopulation has consequences for local biofilm robustness and if/how the distribution of non-producers changes during biofilm development. In fact, biofilms are non-uniform structures with variable and local cell and polymer densities (27), which could be linked to different behavior of cells within a clonal population. Understanding how the heterogeneity of gene expression is linked to both biofilm development and structural robustness would provide better insight into the dynamics of biofilm communities.

The extracellular matrix of *B. subtilis* consists of two major components: an amyloid protein, TasA, and exopolysaccharide (EPS) (28). The EPS component is synthesized by protein products encoded by the *epsA-epsO* operon, with Δ*eps* mutants producing a weak and fragile biofilm (28, 29). The protein component is encoded in the *tapA-sipW-tasA* operon, with Δ*tasA* mutants unable to produce a biofilm (30). Strains lacking both operons cannot form a biofilm, whereas strains producing one of the components can complement each other and produce a wild-type-like pellicle (12, 28, 31). In this study, we demonstrate that, under exposure to shear stress, these seemingly sturdy pellicle biofilms disintegrate into extremely robust aggregates and single cells. We reveal that spatial and temporal changes in biofilm structural heterogeneity correlate with changes in expression of biofilm components, as cells in the ON state dominate within unbreakable biofilm aggregates. Therefore, despite inclusive fitness benefits from sharing the public goods within an isogenic population of producers, phenotypic cooperators (ON cells) still partially privatize the biofilm matrix. Further, we propose that

protein matrix component TasA plays a key role in maintaining biofilm robustness, with major consequences for the timing of development and the overall productivity of the biofilm. In general, our study links changes of phenotypic heterogeneity pattern with different stages of biofilm formation and reveals a fingerprint of such heterogeneity in biofilm structural robustness. It also reveals that privatization of public goods occurs even in isogenic microbial populations.

## RESULTS

**Structural heterogeneity develops in late stages of pellicle growth.** It is well established that mature *B. subtilis* pellicles exhibit phenotypical heterogeneity of matrix gene expression (13, 16, 31). To investigate whether this could translate into non-uniform robustness within the biofilm, which we refer to as "structural heterogeneity", biofilms were mechanically disrupted by vortexing with sterile glass sand (Fig. 1a). Consequently, biofilm cells could be separated into two fractions: a fragile dispersible fraction, and a robust non-dispersible fraction, of which 'clumps' could be easily observed under a microscope with low magnifications and persisted up to 8 days old pellicles. (Fig. 1a). This structural heterogeneity of the biofilm was predominantly observed in mature pellicles and the fractions were dynamic as the pellicle aged (Fig. 1b). During the establishment of a pellicle, around 13–16 h after inoculation of the bacteria into MSgg medium, similar amounts of cells could be found in both robust and fragile fractions. Between 19 and 24 h, the juvenile pellicle was mostly structurally homogenous, as it consist solely of a robust fraction. In later stages of pellicle development, the biofilm was again structurally heterogeneous, with an increase in cell number in the fragile fraction.

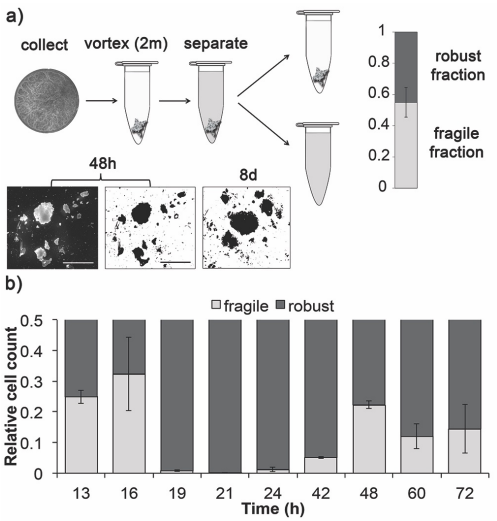


**Fig. 1. Structural heterogeneity in pellicle biofilms.** **a)** Mechanical disruption of biofilms into "robust" and "fragile" fractions by vortexing the pellicle with sterile glass beads. Microscopy images show that the robust fraction consists of non-dispersible clumps that could be observed under a microscope with low magnification. These clumps were also present in 8-day-old pellicles. Scale bars indicate 5 mm. **b)** Temporal changes in relative abundance of cells belonging to the robust and fragile fraction of the biofilm. The blue bar represents the robust fraction, while the yellow bar represents the

fragile fraction. Data represent an average from biological triplicates and error bars correspond to standard errors.

**Temporal changes in structural heterogeneity overlap with changes in phenotypic heterogeneity.** Having shown that structural heterogeneity changes throughout biofilm development, we next sought to determine what underlies these changes. Considering that biofilms are non-uniform structures with variable polymer densities, we chose to investigate the expression of the *epsA-epsO* and *tapA-sipW-tasA* operons encoding the two major components of the biofilm, EPS and amyloid protein TasA, respectively (27, 28). Transcription levels were analyzed by flow cytometry using $P_{eps}$-*gfp* and $P_{tapA}$-*gfp* reporter strains at various pellicle ages (Fig. 2a). Expression of $P_{eps}$-*gfp* was shown to be low at 12 h, when pellicles first emerged, indicating that most cells produced no or very low amounts of EPS. This was followed by a shift in expression around 16 h, with subpopulations present in both the *epsA-epsO* ON and OFF states. At around 24 h, cells were mostly phenotypically homogenous through high expression of the *eps* operon. At later time points, heterogeneity increased once again, with a shift towards lower EPS production. Expression of $P_{tapA}$-*gfp* showed a similar trend, with heterogeneity shifting towards TasA production at early time points, followed by homogeneity around 24 h, and heterogeneity shifting towards the OFF state in older biofilms. We observed similar changes in phenotypic heterogeneity when $P_{eps}$-*gfp* strains were analyzed under a confocal microscope (Fig. 2b,c). Expression of *epsA-epsO* was most prevalent from 19-24 h with OFF subpopulations being observed at earlier and later time points. The changes we observed in phenotypic heterogeneity of *epsA-epsO* and *tapA-sipW-tasA* expression correlated with the temporal changes we observed in structural heterogeneity of the biofilm. This led us to hypothesize a spatial correlation between ON cells and the non-dispersible parts of the biofilm.

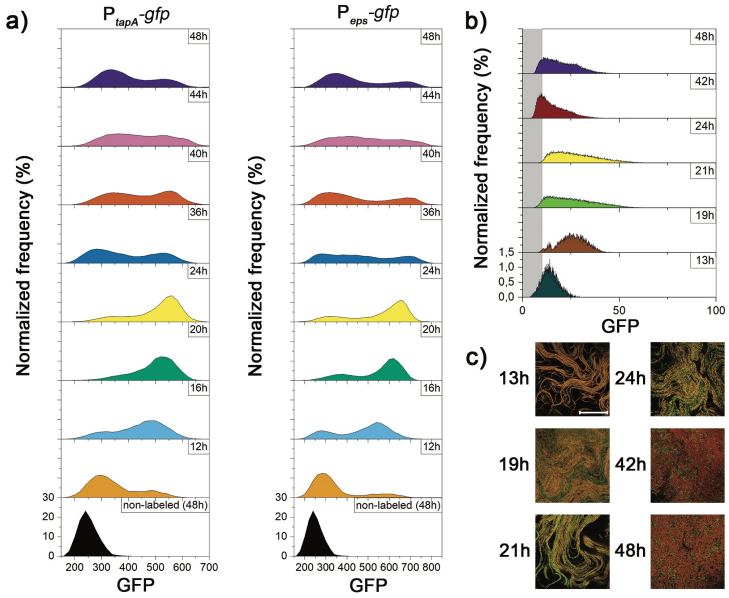


**Fig. 2. Changes in matrix gene expression during biofilm development. a)** Flow cytometry analysis showing average (*n* = 3) distributions of fluorescence intensities of GFP-based transcriptional reporters for *epsA-epsO* (left) and *tapA-sipW-tasA* (right) at various time points throughout biofilm development. **b)** Quantitative assessment of *epsA-epsO* transcriptional GFP reporter inside pellicle biofilms at various developmental stages, based on image cytometry of confocal laser scanning microscopy images. **c)** Cells constitutively expressing mKate2 (OFF cells) are colored magenta, while $P_{epsA}$-GFP expressing cells (ON cells) are colored green. Images show the overlay of magenta and green channels. Scale bar denotes 50 µm.

**Robustness is positively correlated with *epsA-epsO* and *tapA-sipW-tasA* expression.** To investigate if robustness is spatially related to high levels of polysaccharide and amyloid protein production, pellicles established by $P_{eps}$-*gfp* reporter strains were mechanically disrupted after which 'clumps' and dispersible fractions were separately analyzed under a fluorescence microscope (Fig. 3a). Microscopy images showed the presence of both ON and OFF cells in intact pellicles, while ON cells were mostly present in the non-dispersible robust fraction and OFF cells were prevalent in the dispersible fragile fraction. Following this observation, mechanically disrupted pellicles containing $P_{eps}$-*gfp* and $P_{tapA}$-*gfp* reporter strains were analyzed by flow cytometry (Fig. 3b). Pellicle with ages of 24, 36 and 48 h were chosen because of the shift towards phenotypic heterogeneity we had observed as the pellicles aged (see above). At 24 h, expression of both operons was similar in both the fragile and robust fractions, with a slightly higher proportion of ON cells within the robust part of the pellicle. At 36 h, there were

more OFF cells within the fragile fraction and vice versa. This shift in expression was most apparent at 48 h, at which time fewer ON cells were present in the fragile fraction, and a large subpopulation of ON cells was found in the robust fraction. This difference in the amount of ON cells was most evident in the expression of $P_{tapA}$-*gfp.* Additionally, we observed TasA non-producers, cocultured with EPS non-producers, to be dominant at the breakage points of clumps (SI Appendix, Fig. S1), suggesting an involvement of TasA in biofilm integrity. Therefore, we concluded that expression of the *epsA-epsO* operon and especially the *tapA-sipW-tasA* operon positively correlates with the mechanical robustness of the pellicle, with changes in structural and phenotypic heterogeneity of biofilms linked in time and space.

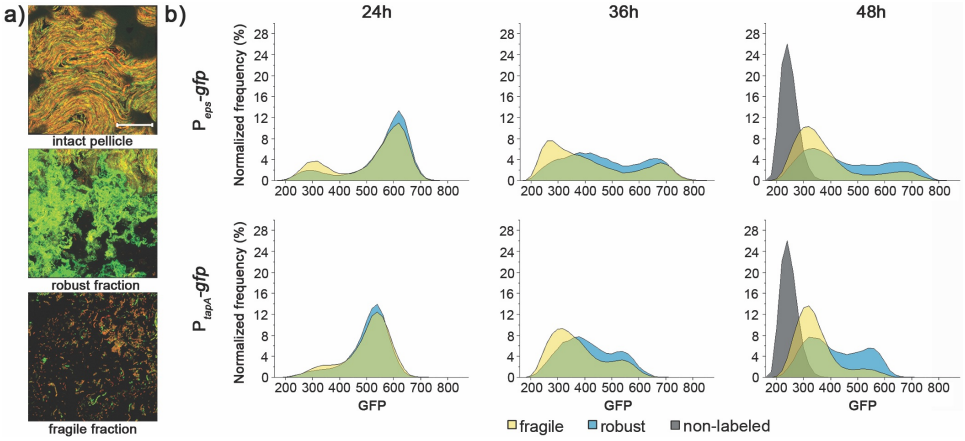


**Fig. 3. Expression of matrix genes in robust and fragile fractions of the biofilm**. **a)** Confocal microscopy images of intact and mechanically disrupted $P_{eps}$-*gfp*, $P_{hyperspank}$-*mKATE2* pellicles. Images show the overlay of magenta and green channels. Scale bar indicates 35 μm. **b)** Flow cytometry analysis showing average ($n$ = 3) distributions of fluorescence intensities of mechanically disrupted $P_{eps}$-*gfp* and $P_{tapA}$-*gfp* reporter strains after 24, 36, and 48 h. The blue histogram represents the robust fraction, while yellow graph represents the fragile fraction; grey graph depicts non-labelled cells.

**TasA non-producers have negative effects on the timing of pellicle development and final pellicle productivity.** Next, we aimed to determine how each matrix component affects biofilm development. First, we competed biofilm mutants lacking one or both matrix components against the wild-type in competition assays with 1:1 relative inoculation. Fig. 4a shows the

selection rate of biofilm mutants in both the liquid medium fraction and in the pellicle after 24 and 48 h. Although Δ*eps* mutant and wild-type strains were equally fit inside the pellicle, the mutant could outcompete wild-type in liquid conditions. On the contrary, the Δ*tasA* mutant could only outcompete the wild-type after 48 h when in liquid and was significantly outcompeted in the pellicle. Furthermore, the Δ*eps*Δ*tasA* mutant was significantly outcompeted in both the pellicle and liquid after 48 h. The exclusion of the Δ*tasA* mutants from pellicle formation suggests it has negative effects on biofilm development. Thus, the effect of biofilm mutants on pellicle productivity (i.e. total number of cells in the pellicle) during development was assessed (Fig. 4b). Cocultures of wild-type and biofilm mutants were mixed 1:1, and colony-forming unit (CFU) productivity in the liquid and pellicle was determined at various time points throughout the development. When the wild-type was mixed with either Δ*eps* or Δ*eps*Δ*tasA* mutants, the timing of pellicle development was similar to that for the wild-type growing alone, with no reduction in final pellicle productivity. By contrast, when the wild-type was mixed with Δ*tasA,* pellicle development was slower and the final pellicle productivity was decreased. A negative effect of Δ*tasA* on the timing of pellicle formation was also confirmed by stereomicroscope time lapse movies (SI Appendix, Fig. S2 and Video S1). In conclusion, TasA non-producers seem to slow down pellicle development and reduce final pellicle productivity. In addition, lack of a negative impact of Δ*eps*Δ*tasA* suggests that EPS production is required for positioning of Δ*tasA* in the pellicle and its negative effects on development and productivity.

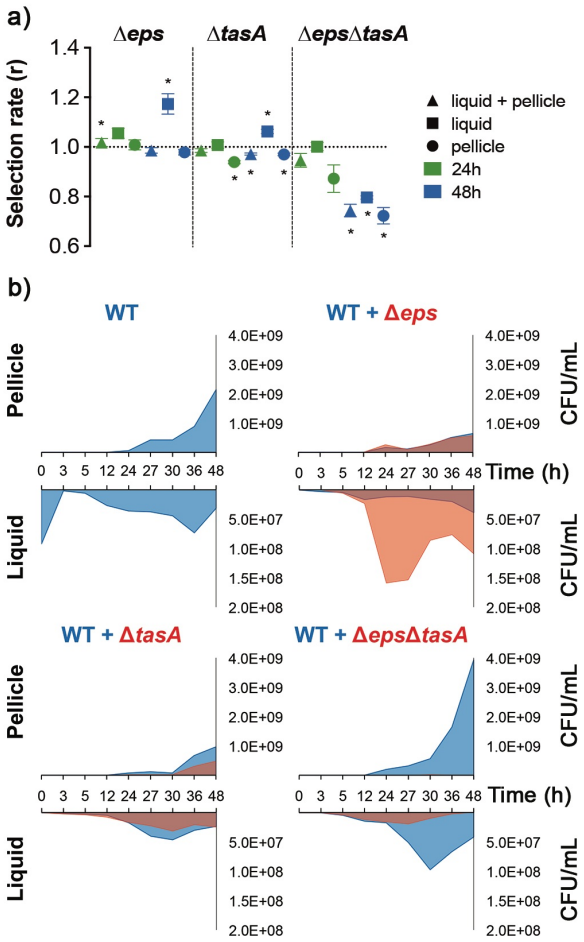


**Fig. 4. Fitness of biofilm mutants in the pellicle and their effect on biofilm development. a)** Selection rate of biofilm mutants in the pellicle and in liquid medium (below the biofilm) measured after 24 h and 48 h based on total colony-forming units (CFU)/ml counts. Each point represents an average of *n*=8 replicates with error bars corresponding to standard errors. **b)** Temporal changes in productivity during biofilm development in wild-type monoculture, and in cocultures of the wild-type with either Δ*eps*, Δ*tasA* or Δ*eps*Δ*tasA* strains. Productivity was assessed at different time points both in the pellicle and in liquid medium (below the biofilm). Each graph represents the average of *n* = 3 biological replicates.

**TasA non-producers diminish pellicle robustness, while EPS non-producers do not.** The function of TasA as a linkage protein and the importance of TasA for pellicle development suggest its significant contribution towards pellicle robustness. To investigate this, cocultures containing increasing percentages of Δ*eps* or Δ*tasA* were mixed with the wild-type and CFU productivity in the robust and fragile fractions of the pellicle was determined (Fig. 5). When the wild-type was confounded with Δ*eps*, wild-type productivity in the robust fraction was reduced but its level was maintained as the proportion of Δ*eps* increased. In contrast, the fragile fraction showed a decrease in, and eventual cease of, the wild-type productivity with increasing percentages of Δ*eps*. In contrast, if the wild-type was mixed with Δ*tasA*, wild-type productivity in the robust fraction decreased and then collapsed as the proportion of Δ*tasA* increased. Similar to Δ*eps*, the fragile fraction showed a decrease in, and eventual cease of, wild-type productivity. These results

clearly show the negative impact of TasA non-producers on pellicle robustness, whereas even at high frequencies of EPS non-producers, a robust pellicle fraction can be maintained.

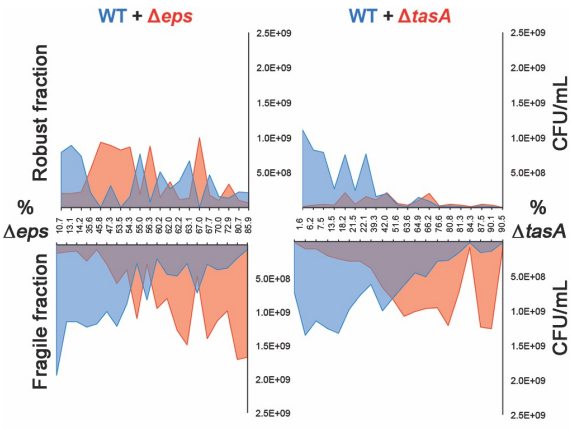


**Fig. 5. Effect of biofilm mutants on pellicle robustness.** Productivities of wild-type and mutants based on total CFU/ml were assessed in mechanically disrupted robust and fragile fractions in cocultures of WT with increasing ratios of either Δ*eps* or Δ*tasA*.

## DISCUSSION

Studies on the social interactions between genetically engineered matrix producers and non-producers have become a gold standard in sociobiology of biofilm communities (11, 31–33). Here, we addressed the consequences of native within-population phenotypic heterogeneity in matrix production for robustness, productivity and timing of biofilm development. We revealed that production of matrix components shifts throughout biofilm development and that these changes correlate with temporal and spatial changes in biofilm robustness.

Biofilm development can be studied from different aspects (34–37). Here, we showed that in the initial stage of biofilm formation, the majority of the population was in an ON state, followed by heterogeneity in older biofilms. This is in line with previous studies, in which the spatiotemporal dynamics patterns of gene expression during the formation of submerged *Escherichia coli* biofilms were investigated (34). Moreover, bimodal expression of curli fibers was demonstrated, with high curli expression being confined to dense cell aggregates. The bimodal spatial expression of the structurally important curli fibers suggests a similar role for TasA, with these higher cell density aggregates providing protection against shear stress.

Furthermore, in another study, the production of curli fibers was shown to protect the biofilm population against bacteriophage (35).

Importantly, cells exhibiting the ON state are more likely to occupy the most robust areas of the biofilm, thereby privatizing the benefit from matrix production under exposure to shear stress. Previous studies have shown that phenotypic heterogeneity of matrix production is present in biofilms of different species (14–16), with a similar phenomenon likely to occur in other biofilm-producing bacteria. Recently, quantitative visualization of *Pseudomonas aeruginosa* aggregates has shown peak alginate gene expression in cells proximal to the surface compared with cells in the interior (38). Although it is likely that the interior of the *B. subtilis* pellicle biofilm contains more OFF cells, we believe that the temporal shift we observed from heterogeneity to homogeneity, then again towards heterogeneity is due to phenotypic differences between randomly distributed isogenic cells.

Accordingly, we revealed that TasA non-producers have adverse effects on the timing of matrix development, productivity and robustness, which was not the case for the EPS non-producers. As EPS is likely costlier to produce and less privatized than TasA (31), the diminishing effects of Δ*tasA* may be linked to the specific structural role of TasA in the matrix, as could also be supported by its distinct localization pattern (39). The dominance of ON cells in the robust biofilm fraction was especially pronounced for *tasA* expression. Furthermore, we observed TasA-non-producers to be dominant at breakage points of biofilm clumps, suggesting these areas are weak points in biofilm integrity.

Conceivably, TasA functions similarly to the structural protein RmbA described in *Vibrio cholerae* biofilms, creating strong linkage between the producing cells (33). If the linkage role holds true, Δ*tasA* cells should be impaired in their ability to integrate into pre-established wild-type pellicles, which will be explored in the future. TasA was shown to have a strong adhesive

role during interspecies interactions (40) and has been linked to structural integrity and physiology of *B. subtilis* biofilms (41, 42).

Our results support previous observations showing the importance of linkage proteins in formation of biofilms (28), as well as the presence of non-uniform biofilm structures (27). It remains to be discovered how extracellular matrix remains privatized by ON cells and what are the ecological consequences or potential evolutionary benefits from biofilm structural heterogeneity. One possibility is bet-hedging where weakly associated cells would adapt for short starvation periods, while early-sporulating aggregates are adapted for longer starvation periods, as proposed for slime molds (43). It remains to be tested, whether robust and fragile fractions of *B. subtilis* biofilms differ in sporulation dynamics.

Our work has four major conclusions: 1) seemingly integral biofilms consist of robust and loosely associated cells, thereby being structurally heterogeneous; 2) changes in the phenotypic heterogeneity pattern of matrix gene expression correlate with changes in biofilm structural heterogeneity in time and space; 3) TasA non-producers have detrimental effects on matrix development and structural integrity; 4) even in clonal microbial populations, where cooperation is stabilized by inclusive fitness benefits, public goods may be partially privatized by phenotypic producers.

## MATERIALS AND METHODS

**Strains and cultivation methods.** Strains used in this study are listed in Table 1. All strains were maintained in lysogeny broth (LB; LB-Lennox, Carl Roth; 10 g/L tryptone, 5 g/L yeast extract and 5 g/L NaCl), while MSgg medium (5 mM potassium phosphate (pH 7), 100 mM MOPS (pH 7), 2 mM $MgCl_2$, 700 µM $CaCl_2$, 50 µM $MnCl_2$, 50 µM $FeCl_3$, 1 µM $ZnCl_2$, 2 µM thiamine, 0.5% glycerol, 0.5% glutamate) was used to induce biofilm formation (20). To obtain pellicle biofilms, bacteria were grown in static liquid MSgg medium at 30°C for 48 h, using 1% inoculum from overnight cultures. Prior to experiments, pellicles were sonicated according to an optimized protocol that allows for disruption of biofilms without affecting cell viability (12, 44). Productivity was determined by plating countable dilutions on LB-agar to obtain CFU levels.

**Structural heterogeneity assay.** To assess structural heterogeneity of biofilms, pellicles were collected and transferred into a 1.5-mL Eppendorf tube containing 1 mL of 0.9% NaCl and ca. 20 µL of sterile glass sand (Carl Roth). Next, pellicles were vortexed (Scientific Industries, Vortex-Genie 2) for 2 min and pellicle debris was allowed to sediment for 5 minutes. The dispersible fraction was transferred to a new Eppendorf tube, while the non-dispersible 'clumps' fraction was diluted in 1 mL of 0.9% NaCl. Both fractions were sonicated as described previously (12), after which CFU levels were determined.

**Fitness assays.** To determine the fitness costs of EPS and TasA production, mKATE2-labeled wild-type strains were competed with various biofilm-formation mutants. Overnight cultures were adjusted to the same optical density (OD), mixed at a 1:1 ratio, and 1% coculture inoculum was transferred into 1.5 mL MSgg medium. Cocultures were grown in static conditions at 30°C. CFU levels in both sonicated pellicle and liquid medium were determined immediately after inoculation and after 24 or 48 h of growth. Wild-type colonies were

distinguished from biofilm mutants based on pink color (visible emission from mKate2 reporter). The selection rate (r) was calculated as the difference in the Malthusian parameters of both strains: r = ln[mutant (t=1)/mutant (t=0)]-(ln[wild-type(t=1)/wild-type(t=0)]), where t=1 is the time point at which the pellicle was harvested (45).

**Flow cytometry.** To analyze expression levels of the *epsA-epsO* and *tapA-sipW-tasA* operons, flow cytometry analysis was performed using a BD FACScanto II (BD Biosciences). Three replicates per condition were incubated at 30°C for 12, 16, 20, 24, 36, 40, 44, or 48 h. Afterwards, pellicles were harvested and sonicated. To study structural heterogeneity, harvested pellicles were vortexed as previously described, before sonication. Pellicles that were 12, 16, 20 or 24 h-old were diluted 20 times, whereas pellicles that were 36, 40, 44, or 48 hours old were diluted 200 times before flow cytometry analysis was performed. To obtain the average distribution of expression levels between replicates, data obtained from each replicate were subjected to binning using an identical bin size. Next, a mean count for each bin was obtained by averaging individual counts within this bin across all replicates, resulting in the mean distribution of single-cell level expression per condition.

**Microscopy.** To observe how biofilm mutants affect biofilm development, time lapse microscopy experiments were performed. Overnight cultures were adjusted to the same optical density (OD), mixed in a 1:3 ratio (wild-type:mutant), and inoculated in 500 µL MSgg medium inside an 8-well tissue culture chamber at 30°C (Sarstedt; width: 24 mm, length: 76 mm, growth area: 0.8 $cm^2$). Bright-field images of pellicles were taken with an Axio Zoom V16 stereomicroscope (5x magnification; Carl Zeiss, Jena, Germany) equipped with a Zeiss CL 9000 LED light source, and an AxioCam MRm monochrome camera (Carl Zeiss), in which exposure time was set to 35 ms and images were captured every 15 minutes for a total of 48 h.

Additionally, time-lapse videos of the wild-type monoculture biofilm development were recorded. For quantitative assessment of phenotypic heterogeneity, $P_{eps}$-*gfp* pellicles were analyzed using a confocal laser scanning microscope (LSM 780, Carl Zeiss) equipped with a Plan-Apochromat/1.4 Oil DIC M27 63× objective and an argon laser (excitation at 488 nm for green fluorescence and 561 nm for red fluorescence, emission at 528 (±26) nm and 630 (±32) nm respectively). Zen 2012 Software (Carl Zeiss) and FIJI Image J Software (46) were used for image recording and subsequent processing, respectively.

**Image analysis.** Strain frequencies were quantified from confocal microscopy images using our recently developed BiofilmQ software (47). This analysis involved the registration of image time series to avoid sample drift, followed by top-hat filtering to eliminate noise, and Otsu thresholding to obtain a binary segmented image that separates the biofilm 3D location from the background. Using the BiofilmQ-inbuilt technique for dissecting this 3D volume into pseudo-cell cubes, which have the same volume as an average *B. subtilis* cell, we quantified the relative and absolute abundances of strains in different fluorescence channels at different time points.

**ACKNOWLEDGEMENTS**

This work was funded by the Deutsche Forschungsgemeinschaft (DFG) to Á.T.K. (KO4741/2.1) within the Priority Program SPP1617, and the Collaborative Research Center SFB987 (to K.D.). S.B.O. and M. M. were supported by an Erasmus+ fellowship and a FEMS Research and Training Grant (FEMS-RG-2017-0054), respectively. This project has received funding from the European Union's Horizon 2020 research and innovation programme under the Marie Skłodowska-Curie grant agreement No 713683 (H.C. Ørsted COFUND to A.D.) and the European Research Council (StG-716734 to K.D.). Work in the laboratory of Á.T.K. is partly supported by the Danish National Research Foundation (DNRF137) for the Center for Microbial Secondary Metabolites.

**Competing Interests**

The authors declare that there are no competing financial interests in relation to the work described.

**Authors contributions**

Á.T.K. and A.D. conceived the project; S.B.O., M.M., D.S., R.H., and A.D. performed experiments; K.D. and S.B. contributed methodologies and equipment, respectively; S.B.O, A.D. and Á.T.K. wrote the manuscript, with all authors contributing to the final version.

**REFERENCES**

1. López D, Vlamakis H, Kolter R (2010) Biofilms. *Cold Spring Harb Perspect Biol* 2:a000398.
2. Hall-Stoodley L, Stoodley P (2009) Evolving concepts in biofilm infections. *Cell Microbiol* 11:1034–1043.
3. Rochex A, Godon JJ, Bernet N, Escudié R (2008) Role of shear stress on composition, diversity and dynamics of biofilm bacterial communities. *Water Res* 42:4915–4922.
4. Stewart PS (2002) Mechanisms of antibiotic resistance in bacterial biofilms. *Int J Med Microbiol* 292:107–113.
5. Hamilton WD (1964) The genetical evolution of social behaviour. I. *J Theor Biol* 7(1):1–16.
6. West SA, Diggle SP, Buckling A, Gardner A, Griffin AS (2007) The social lives of microbes. *Annu Rev Ecol Evol Syst* 38:53–77.
7. West S a., Griffin AS, Gardner A (2007) Evolutionary explanations for cooperation. *Curr Biol* 17:661–672.

8. Hardin G (1968) The tragedy of the commons. *Science (80- )* 162(June):1243–1248.
9. West SA, Griffin AS, Gardner A, Diggle SP (2006) Social evolution theory for microorganisms. *Nat Rev Microbiol* 4:597–607.
10. Rainey PB, Rainey K (2003) Evolution of cooperation and conflict in experimental bacterial populations. *Nature* 425:72–74.
11. Drescher K, Nadell CD, Stone HA, Wingreen NS, Bassler BL (2014) Solutions to the public goods dilemma in bacterial biofilms. *Curr Biol* 24:50–55.
12. Martin M, et al. (2017) *De novo* evolved interference competition promotes the spread of biofilm defectors. *Nat Commun* 8:15127.
13. Martin M, Dragoš A, Schäfer D, Maróti G, Kovács ÁT (2018) Cheater-mediated evolution shifts phenotypic heterogeneity in *Bacillus subtilis* biofilms. *bioRxiv*:494716.
14. Grantcharova N, Peters V, Monteiro C, Zakikhany K, Römling U (2010) Bistable expression of CsgD in biofilm development of *Salmonella enterica* serovar *typhimurium*. *J Bacteriol* 192:456–466.
15. Cárcamo-Oyarce G, Lumjiaktase P, Kümmerli R, Eberl L (2015) Quorum sensing triggers the stochastic escape of individual cells from *Pseudomonas putida* biofilms. *Nat Commun* 6:5945.
16. Chai Y, Chu F, Kolter R, Losick R (2008) Bistability and biofilm formation in *Bacillus subtilis*. *Mol Microbiol* 67:254–263.
17. Rudrappa T, Biedrzycki ML, Bais HP (2008) Causes and consequences of plant-associated biofilms. *FEMS Microbiol Ecol* 64:153–166.
18. Vaseeharan B, Ramasamy P (2003) Control of pathogenic *Vibrio* spp. by *Bacillus subtilis* BT23, a possible probiotic treatment for black tiger shrimp *Penaeus monodon*. *Lett Appl Microbiol* 36:83–87.
19. Avery S V. (2006) Microbial cell individuality and the underlying sources of heterogeneity. *Nat Rev Microbiol* 4:577–587.
20. Branda SS, González-Pastor JE, Ben-Yehuda S, Losick R, Kolter R (2001) Fruiting body formation by *Bacillus subtilis*. *Proc Natl Acad Sci U S A* 98(20):11621–11626.
21. Hölscher T, et al. (2015) Motility, chemotaxis and aerotaxis contribute to competitiveness during bacterial pellicle biofilm development. *J Mol Biol* 427:3695–3708.
22. Vlamakis H, Chai Y, Beauregard P, Losick R, Kolter R (2013) Sticking together: Building a biofilm the *Bacillus subtilis* way. *Nat Rev Microbiol* 11(3):157–168.
23. Gilbert OM, Foster KR, Mehdiabadi NJ, Strassmann JE, Queller DC (2007) High relatedness maintains multicellular cooperation in a social amoeba by controlling cheater mutants. *Proc Natl Acad Sci* 104:8913–8917.
24. Inglis RF, Ryu E, Asikhia O, Strassmann JE, Queller DC (2017) Does high relatedness promote cheater-free multicellularity in synthetic lifecycles? *J Evol Biol* 30:985–993.
25. Ho HI, Hirose S, Kuspa A, Shaulsky G (2013) Kin recognition protects cooperators against cheaters. *Curr Biol* 23:1590–1595.
26. Stefanic P, Kraigher B, Lyons NA, Kolter R, Mandic-Mulec I (2015) Kin discrimination between sympatric *Bacillus subtilis* isolates. *Proc Natl Acad Sci* 112:14042–14047.
27. Stewart PS, Murga R, Srinivasan R, de Beer D (1995) Biofilm structural heterogeneity visualized by three microscopic methods. *Water Res* 29:2006–2009.
28. Branda SS, Chu F, Kearns DB, Losick R, Kolter R (2006) A major protein component of the *Bacillus subtilis* biofilm matrix. *Mol Microbiol* 59:1229–1239.
29. Kearns DB, Chu F, Branda SS, Kolter R, Losick R (2005) A master regulator for biofilm formation by *Bacillus subtilis*. *Mol Microbiol* 55(3):739–749.
30. Romero D, Vlamakis H, Losick R, Kolter R (2011) An accessory protein required for anchoring and assembly of amyloid fibres in *B. subtilis* biofilms. *Mol Microbiol* 80:1155–

1168.
31. Dragoš A, et al. (2018) Division of labor during biofilm matrix production. *Curr Biol* 28:1903–1913.
32. Yan J, Nadell CD, Stone HA, Wingreen NS, Bassler BL (2017) Extracellular-matrix-mediated osmotic pressure drives *Vibrio cholerae* biofilm expansion and cheater exclusion. *Nat Commun* 8:327.
33. Nadell CD, Drescher K, Wingreen NS, Bassler BL (2015) Extracellular matrix structure governs invasion resistance in bacterial biofilms. *ISME J* 9:1700–1709.
34. Besharova O, Suchanek VM, Hartmann R, Drescher K, Sourjik V (2016) Diversification of gene expression during formation of static submerged biofilms by *Escherichia coli*. *Front Microbiol* 7:1568.
35. Vidakovic L, Singh PK, Hartmann R, Nadell CD, Drescher K (2017) Dynamic biofilm architecture confers individual and collective mechanisms of viral protection. *Nat Microbiol* 3:26–31.
36. Srinivasan S, et al. (2018) Matrix production and sporulation in *Bacillus subtilis* biofilms localize to propagating wave fronts. *Biophys J* 114:1490–1498.
37. Pisithkul T, et al. (2019) Metabolic remodeling during biofilm development of *Bacillus subtilis*. *MBio* 10:e00623-19.
38. Jorth P, Spero AM, Newman KD (2019) Quantitative visualization of gene expression in *Pseudomonas aeruginosa* aggregates reveals peak expression of alginate in the hypoxic zone. *bioRxiv* doi:10.1101/632893.
39. van Gestel J, Vlamakis H, Kolter R (2015) From cell differentiation to cell collectives: *Bacillus subtilis* uses division of labor to migrate. *PLoS Biol* 13:e1002141.
40. Duanis-Assaf D, et al. (2018) Cell wall associated protein TasA provides an initial binding component to extracellular polysaccharides in dual-species biofilm. *Sci Rep* 8:9350.
41. Romero D, Aguilar C, Losick R, Kolter R (2010) Amyloid fibers provide structural integrity to *Bacillus subtilis* biofilms. *Proc Natl Acad Sci* 107:2230–2234.
42. Cámara-Almirón J, et al. Dual functionality of the TasA amyloid protein in *Bacillus* physiology and fitness on the phylloplane. *bioRxiv* doi:10.1101/651356.
43. Tarnita CE, Washburne A, Martinez-Garcia R, Sgro AE, Levin SA (2015) Fitness tradeoffs between spores and nonaggregating cells can explain the coexistence of diverse genotypes in cellular slime molds. *Proc Natl Acad Sci* 112:2776–2781.
44. Dragoš A, et al. (2018) Evolution of exploitative interactions during diversification in *Bacillus subtilis* biofilms. *FEMS Microbiol Ecol* 94:fix155.
45. Travisano M, Lenski RE (1996) Long-term experimental evolution in *Escherichia coli*. IV. Targets of selection and the specificity of adaptation. *Genetics* 143(1):15–26.
46. Rueden CT, et al. (2017) ImageJ2: ImageJ for the next generation of scientific image data. *BMC Bioinformatics* 18:529.
47. Hartmann R, et al. BiofilmQ, a software tool for quantitative image analysis of microbial biofilm communities. *bioRxiv*:https://doi.org/10.1101/735423v1.
48. Konkol MA, Blair KM, Kearns DB (2013) Plasmid-encoded comI inhibits competence in the ancestral 3610 strain of *Bacillus subtilis*. *J Bacteriol* 195(18):4085–4093.
49. Hölscher T, et al. (2016) Monitoring spatial segregation in surface colonizing microbial populations. *J Vis Exp* 2016(116):e54752.
50. Mhatre E, et al. (2017) Presence of calcium lowers the expansion of *Bacillus subtilis* colony biofilms. *Microorganisms* 5:7.

**Table 1.** Strains used in this study

| Strain | Genotype | Reference |
|---|---|---|
| DK1042 | 3610 *comI*$^{Q12I}$ (wild type) | (48) |
| TB35 | 3610 *comI*$^{Q12I}$ *amyE::*$P_{hyperspank}$-mKate2 ($Cm^R$) | (49) |
| TB864 | 3610 *comI*$^{Q12I}$ *amyE::*$P_{hyperspank}$-mKate2 ($Cm^R$) *sacA::*$P_{eps}$-*gfp* ($Km^R$) | (44) |
| TB865 | 3610 *comI*$^{Q12I}$ *amyE::*$P_{hyperspank}$-mKate2 ($Cm^R$) *sacA::*$P_{tapA}$-*gfp* ($Km^R$) | (44) |
| TB501 | 3610 *comI*$^{Q12I}$ *amyE::*$P_{hyperspank}$-mKate2 ($Spec^R$) | (44) |
| TB601 | 3610 *comI*$^{Q12I}$ *eps::*$Tet^R$ | (44) |
| TB602 | 3610 *comI*$^{Q12I}$ *tasA::*$Spec^R$ | (50) |
| TB863 | 3610 *comI*$^{Q12I}$ *tasA::*$Km^R$ | (31) |
| TB852 | 3610 *comI*$^{Q12I}$ *eps::*$Tet^R$, *tasA::*$Km^R$ | This study |

TB852 was obtained by transforming DK1042 with gDNA isolated from TB601 and TB863, and selecting for tetracycline and kanamycin-resistant colonies, respectively. $Cm^R$, $Spec^R$, $Km^R$, and $Tet^R$ denote chloramphenicol, spectinomycin, kanamycin, and tetracycline resistance cassettes, respectively.